Pis'ma v ZhETF, vol.66, iss.12, pp.787 - 792

OBSERVATION OF THE PLASMA CHANNEL DYNAMICS AND COULOMB EXPLOSION IN THE INTERACTION OF A HIGH INTENSITY LASER PULSE WITH HE GAS JET

G.S.Sarkisov[1)], *V.Yu.Bychenkov, V.T.Tikhonchuk, A.Maksimchuk*, S.Y.Chen*, R.Wagner*, G.Mourou*, D.Umstadter**

P.N.Lebedev Physics Institute RAS
117924 Moscow, Russia

**Center for Ultrafast Optical Science, University of Michigan*
MI 48109-2099, Ann Arbor, USA

Submitted 11 November 1997

We report on first interferometric observations of the dynamics of electron-ion cavitation of relativistically self-focused intense 4 TW 400 fs laser pulse in a He gas jet. The electron density in the channel 1 mm long and 30 μm in diameter drops approximately 10 times from the maximum value of $\sim 8 \cdot 10^{19}$ cm^{-3}. High radial velocity of the plasma expansion $\sim 3.8 \cdot 10^8$ cm/s corresponding to the ion energy about 300 keV has been observed. The total energy of fast ions is estimated to be 6% of the laser pulse energy. The high velocity radial plasma expulsion is explained by a charge separation due to the strong ponderomotive force. This experiment demonstrates a new possibility for direct transmission of a significant part of laser pulse energy into the ions.

PACS: 52.35.Mw, 52.40.Nk, 52.75.Di

A number of proposed applications of ultra-high intensity short laser pulses implies laser guiding for distances much longer than the Rayleigh length. Guiding of intense laser pulses in underdense plasmas due to the relativistic self-focusing has been first reported in Ref. [1] and then studied in details in Refs. [2–6]. However the dynamics of plasma channel at high laser intensities and phenomena associated with its expansion are not addressed yet. This letter presents new experimental results and their theoretical interpretation on the dynamics of the plasma channel produced by a ultra-high intensity, short laser pulse.

The experiment has been performed using the 10 TW Ti:sapphire-Nd:glass laser system based on chirped-pulse amplification [7] developed at the Center for Ultrafast Optical Science, University of Michigan. Laser operates on the wavelength $\lambda = 1.053\,\mu$m and produces 3 J, 400 fs FWHM pulses with the intensity contrast of 10^5. The 50 mm diameter laser beam was focused with an off-axis parabolic mirror ($f/3.3$, f =16.5 cm) to a 10 μm spot with a vacuum intensity $6 \cdot 10^{18}$ W/cm^2. Laser beam was focused in a high backing pressure (7 MPa) He gas jet expanding through a 1 mm diameter nozzle. The optimal conditions for beam guiding correspond to the laser focusing on the jet edge with He atom density $n_{\mathrm{He}} \simeq 3 \cdot 10^{19}$ cm^{-3}. The jet thickness was about 1 mm. A two-channel optical setup has been used for simultaneous recording of interferometric and shadow plasma images. The probe beam was split from the main beam, propagated through an adjustable optical delay, and incident on a plasma in the direction perpendicular to the interaction beam. The plasma was imaged using a single spherical lens with angular aperture $\pm 7°$ on two 12-bit cooled CCD cameras. The spatial and temporal resolution

[1)] e-mail: sarkisov@sci.lebedev.ru

was 10 μm and 400 fs, respectively. For the electron density measurements the air-wedge shearing interferometer [8] was used.

The plasma evolution has been investigated at the time interval from -2 to $+55$ ps. For $t = 0$ is taken the time of arrival of the maximum laser intensity in the focal plane $z = 0$. The first signs of gas ionization were observed at $t = -2$ ps. This indicates the laser intensity is above the He ionization threshold, $\sim 10^{15}$ W/cm^2, at that time [9]. We observed a fast gas ionization in the cone of laser convergence which is 8.6°. It propagates along the laser axis approximately with the velocity of light until it reaches the rear side of the jet. On the time of ionization (from -2 to $+3$ ps) the front part of interferogram is blurred because of the fringe motion during the exposition time. The first signatures of plasma channel formation (fringe bending on the laser axis) were observed at $t = 0$ ps. The channel length increases with sublight velocity up to 1000 μm.

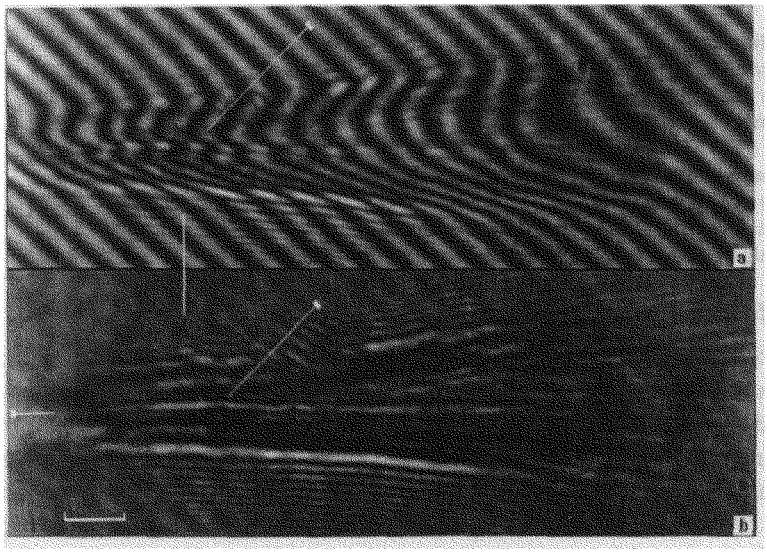

Fig.1. Interferometric (a) and shadow (b) images of a plasma at time 20 ps after focusing 1.7 J, 4.3 TW laser pulse. The 100 μm spatial scale is shown in left corner. Vertical line in the shadow image marks the position of focal plane. Arrows indicate the plasma channel. Horizontal arrow indicates the direction of the interaction laser beam

The interferometric and shadow plasma images taken at $t = 20$ ps are shown in Fig.1 for the laser energy 1.7 J (4.3 TW). Local opposite displacement of the interference fringes in the narrow axial region in the interferogram indicates the decrease of the phase shift in this region and hence the decrease of electron density. This region is manifested in the shadow image by a bright narrow line, that is due to the refraction of probe beam on the high radial electron density gradient. The two-dimensional reconstruction of electron density profile for $t = 35$ ps (assuming the axial symmetry of a plasma) for the same laser conditions is presented in Fig.2a. The maximum electron density is $7.6 \cdot 10^{19}$ cm^{-3} at the radius $\simeq 20\,\mu$m and the depth of the plasma channel is up to 80 – 90%. The accuracy of measurement of the channel depth is limited by the Abel inversion procedure.

The dynamics of electron density profile near the focal plane ($z = 100\,\mu$m) is shown in Fig.2b. The electron density gradient at channel walls reaches the value of $5 \cdot 10^{22}$ cm^{-4} at time 7 ps and remains practically the same up to time 55 ps. The evolution of linear electron density (number of electrons per unit length $N_e = 2\pi \int r dr n_e(r)$) at $z = 100\,\mu$m and the evolution of mean electron density in the same cross-section are presented in Fig.3a. After the initial phase of fast ionization (from -2 to 0 ps) the number of electrons remains constant (from 0 to 9 ps), then an ionization starts again.

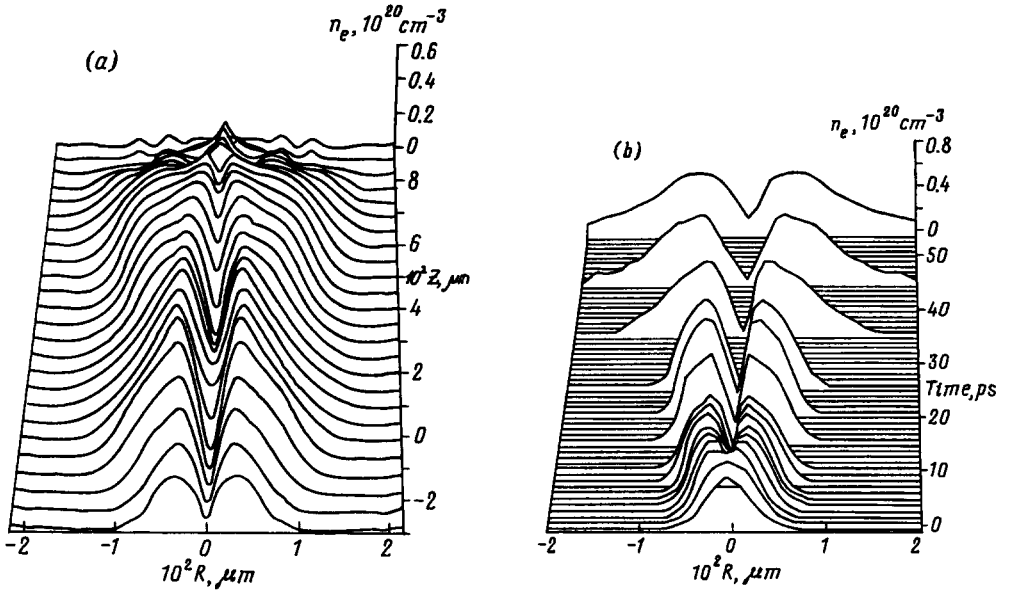

Fig.2. Two-dimensional electron density distribution, $n_e(r, z)$, at time 30 ps (a), and the evolution of the radial electron density profile, $n_e(r, t)$, at the axial position $z = 100\,\mu$m from the focus (b)

At the same time the average electron density starts to decrease. These features are in an agreement with the temporal behavior of plasma radius at $z = 100\,\mu$m) shown in Fig.3b. It remains approximately the same from 0 to 9 ps then plasma begins to expand radialy with almost constant velocity. If we define the plasma edge as a region where the electron density equals $5 \cdot 10^{18}$ cm^{-3} (17% ionization) then the expansion velocity equals to $3.8 \cdot 10^8$ cm/s (curve *1* in Fig.3b). The area of higher degree ionization, $1.5 \cdot 10^{19}$ cm^{-3} (50% ionization), expands with lower velocity $\sim 2.5 \cdot 10^8$ cm/s (curve *2* in Fig.3b).

We attribute the plasma expansion to the ambient gas ionization by fast ions expelled from the channel. Then the expansion of plasma edge (with 17% ionization) can be related to the propagation of fast ions with the energy about 300 keV while the main plasma volume expansion (with 50% ionization) corresponds to 130 keV ions. This assumption of the gas collisional ionization by fast ions explains also $\sim$ 10 ps delay time, which is the time needed for fast ions to penetrate through the laser ionized plasma volume and reach the ambient gas. (The velocity of plasma profile with given density is lower than the actual ion velocity due to the radial ion expansion and decrease of the ion flux. However we neglect this difference in present paper and, therefore, underestimate the ion energy.)

The channel diameter (Fig.3b) also changes with time. Up to time $t = 9$ ps we do not observe a significant variation of channel diameter $D \sim 10 - 15\,\mu$m which is at the limit of our spatial resolution. At $t > 9$ ps the channel diameter increases up to $25 - 35\,\mu$m with a velocity about $6 \cdot 10^7$ cm/s.

The initial laser beam channeling can be attributed to the effect of relativistic self-focusing of intense laser pulse [1]. The critical power for relativistic self-focusing $P_c = 17 n_c/n_e$ GW (where n_e is the electron density and n_c is the critical density) corresponds in our conditions to 280 GW, which is more than 10 times below the actual laser power. Therefore we speculate that the substantial part of laser power is trapped in a narrow

channel near the laser axis. The amount of trapped power depends on the focusing conditions and it is about 50% in the present case. This estimate is deduced from the measurement of the radial energy distribution in the output plane of laser channel. The actual diameter of laser channel is probably smaller than the instrumental resolution and was not measured directly in the experiment. (We estimate the channel radius, $r_0 \approx 3\,\mu$m, below by relating it to the fast ions energy.) The rest of laser power is not trapped and ionizes gas in the laser convergence cone. The measured initial fully ionized plasma radius in the focal plane is $r_p \simeq 40\,\mu$m.

The laser pulse exerts a radial ponderomotive force on electrons, expels them from the axis, and forms an electron channel. It depth, $\delta n_e/n_e = \lambda_e^2 \nabla_r^2 \sqrt{1+a^2/2}$, is about 10% for the laser channel radius $r_0 \approx 3\,\mu$m and $a^2 \approx 5$. This formula follows from the Poisson's equation and the balance between the electrostatic and ponderomotive potentials. Here $\lambda_e = c/\omega_p$ is the electron inertia length, ω_p is the electron plasma frequency, and $a = 0.85 \cdot 10^{-9}\,\lambda[\mu\text{m}]\sqrt{I\,[\text{W/cm}^2]}$ is the dimensionless laser field vector potential in a channel. Ions do not have time to move during the passage of laser pulse and electrons return back to their original position when the pulse ends. However the laser pulse supports the electron channel and because of that looses its energy for ion acceleration. Then the ions in the trace of laser pulse acquire a kinetic energy and begin to move in radial direction. This effect known as "Coulomb explosion" [10] has been discussed as a mechanism of plasma channel formation [4, 5].

For a relatively short laser pulse, $\tau < r_0/u_i \sim 1$ ps, the velocity acquired an ion (with the mass M) from the laser pulse can be estimated as $u_i = (Z/M)mc^2\nabla_r \int dt\sqrt{1+a^2/2}$. Then one finds the ion kinetic energy

$$\epsilon_i = \frac{Z^2}{2M} m^2 c^4 \left(\nabla_r \int dt \sqrt{1+\frac{a^2}{2}} \right)^2, \qquad (1)$$

and the corresponding pulse energy loss per unit length, $d\mathcal{E}/dz \simeq -2\pi \int r dr n_i \epsilon_i$. According to the observations there is a characteristic maximum energy of the ions $\sim$ 300 keV. Formula (1) also predicts the high energy cutoff. For estimates we assume a Gaussian pulse shape in time and over the radius, $I = I_{max}\exp(-t^2/\tau^2 - r^2/r_0^2)$, with $\tau \simeq 240$ fs. Then to accommodate the maximum ion energy of 300 keV with 50% laser energy trapping in the channel, the laser channel radius in Eq. (1) has to be $r_0 \simeq 3\,\mu$m that defines the maximum laser intensity, $I_{max} \sim 8.3 \cdot 10^{18}$ W/cm^2. These estimates of the channel radius and laser intensity qualitatively agree with the theory of relativistic self-focusing [1, 11]. The group of fast $\sim$ 300 keV ions is responsible for the preionization of ambient gas (cf. Fig.3*b*, curve *1*). Eq.(1) predicts a rather wide energy spectrum of the ions with mean energy $\sim$ 130 keV. These ions are initially concentrated in a cylinder with the radius $R \sim 5\,\mu$m and then begin to expand radially. These ions are responsible for the main body ambient gas ionization (50%, cf. Fig.3*b*, curve *2*). The characteristic energy deposited into these ions is $d\mathcal{E}/dz \sim 0.5$ J/cm, which constitutes about 6% of laser pulse energy trapped in the channel of 1 mm length.

There are also relatively low energy ions (about 10 keV) expelled from a larger radius, $r_{ch} \approx 15\,\mu$m which are responsible for the slow dynamics of plasma channel. They are accelerated by the low intensity wings of untrapped part of the laser beam. According to Eq. (1), the intensity required for acceleration of these ions is below 10^{18} W/cm^2.

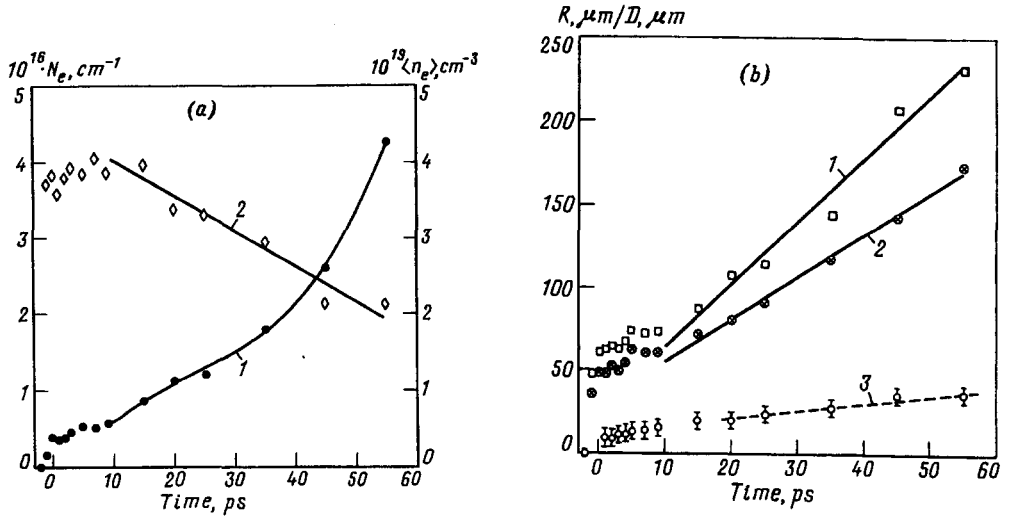

Fig.3. (*a*) Temporal evolution of the linear electron density, $N_e(t)$, (curve *1*) and the mean electron density (*2*) in the cross-section $z = 100\,\mu$m from the focal plane. (*b*) Temporal evolution of the plasma radius at $z = 100\,\mu$m for the $n_e = 5 \cdot 10^{18}$ cm^{-3} (*1*) and $1.5 \cdot 10^{19}$ cm^{-3} (*2*), and the temporal evolution of the plasma channel diameter (*3*)

This regime of plasma channel formation due to the ion acceleration ("Coulomb explosion" according to the terminology of Ref. [10]) is completely different from the mechanism of plasma thermal heating and the electron impact ionization. In the latter case plasma expands with the ion acoustic velocity [2]. The electron temperature, T_e, can be estimated as about 100 eV, according the measurements of Ref. [5] for conditions similar to the present experiment. Therefore the ion acoustic velocity $c_s = \sqrt{ZT_e/M} \sim 7 \cdot 10^6$ cm/s in our experiment is more than 10 times less the ion expansion velocity. We also disagree with the conclusion of Ref. [5] on the plasma expansion with ion acoustic velocity since the conditions of that experiment are similar to ours.

Initially the accelerated ions propagate through a plasma ($R < r_p \sim 40\,\mu$m) and cannot be seen with our diagnostic tools. After the delay time $t_d = r_p/u_i \sim 10$ ps they penetrate into the neutral gas ($r > r_p$) and begin to ionize it. Although the ionization consumes a negligible part of ion energy, it proceeds very efficiently because the fast ion velocity, $u_i \sim (2-4) \cdot 10^8$ cm/s, is comparable to the velocity of bounded electrons in helium atom. These conditions correspond to the maximum of the ionization cross-section $\sigma_i \sim 3 \cdot 10^{-16}$ cm^2 [13]. It is about an order of magnitude larger than the cross-section of He ionization due to the electron collisions.

The electron density at the radius r behind the group of fast ions can be estimated as $n_e \approx n_{He}^2 r_0^2 \sigma_i / r$. This corresponds to about 10% ionization at $r \sim 100\,\mu$m. The degree of preionization decreases with r as the fast ion flux decreases. The 100 eV electrons that accompany fast ions can also contribute to the gas ionization at the level of few percent. According the same formula, the main body 130 keV ions that penetrate in the preionized gas somewhat later produce three times higher ionization at the same distance. Thus one may expect about 50% ionization for $r \sim 100\mu$m that agrees with experimental results. The total number of the electrons behind the ion front increases linearly with time, while

the average electron density is inversely proportional to t. All these qualitative relations as well as the number of the electrons agree with data shown in Fig.3*a*.

In conclusion, the temporal evolution of the plasma channel created due to the relativistic self-focusing of 4 TW 400 fs laser pulse has been observed for the first time using the interferometric technique with high spatial and temporal resolution. By the comparison of experimental data with theoretical estimates we demonstrate that the channel evolution is dominated by the Coulomb explosion effect with subsequent penetration of high energy ions into the ambient neutral gas. This experiment reveals a new efficient mechanism of direct deposition of the laser energy into the high energy ions ($\sim$ 6% for our conditions) which can play a fundamental role in the absorption short, high intensity laser pulses. We estimate the fast ion energy $\sim$ 300 keV or 80 keV/nucleon that is comparable to that observed in the solid target experiment [14].

The authors would like to acknowledge Dr. S. Pikuz for useful discussion. This work was supported by NSF PHY 972661, NSF STC PHY 8920108, DOE/LLNL subcontract B307953, and the Russian Basic Research Foundation (grants 96-02-16707-a and 96-02-16165-a).

---

1. A.B.Borisov, A.V.Borovskiy, V.V.Korobkin et al., Phys. Rev. Lett. **68**, 2309 (1992).
2. M.Dunne, T.Afshar-Rad, J.Edwards et al., Phys. Rev. Lett. **72**, 1024 (1994).
3. A.J.MacKinnon, M.Borgesi, A.Iwase et al., Phys. Rev. Lett. **76**, 1473 (1996); M.Borghesi, A.J.MacKinnon, L.Barringer et al., Phys. Rev. Lett. **78**, 879 (1997).
4. D.Umstadter, S.Y.Chen, A.Maksimchuk et al., Science, **273**, 472 (1996).
5. K.Krushelnik, A.Ting, C.I.Moore et al., Phys. Rev. Lett. **78**, 4047 (1997).
6. V.Malka, E.Wispelaere, F.Amiranoff, S.Baton, Phys. Rev. Lett. **79**, 2979 (1997).
7. P. Maine, D.Strickland, P.Bado et. al., IEEE J. Quantum Electron. **24**, 398 (1988); M.D.Perry and G.Mourou, Science **264**, 917 (1994).
8. G.S.Sarkisov, Instruments and Exp. Tech. **39**, 727 (1996).
9. S.Augst, D.Strickland, D.D.Meyerhofer et al., Phys. Rev. Lett. **63**, 2212 (1989).
10. N.H.Burnett and G.D.Enright, IEEE J. Quant. Electron. **26**, 1797 (1990).
11. P.Sprangle, E.Esarey, J.Krall, G.Joyce, Phys. Rev. Lett. **69**, 2200 (1992); K.C.Tzeng, W.B.Mori, C.D.Decker, Phys. Rev. Lett. **76**, 332 (1996); P.Mora and T.M.Antonsen, Phys. Plasmas **4**, 217 (1997).
12. T.E.Glover, T.D.Donnelly, E.A.Lipman et al., Phys. Rev. Lett. **73**, 78 (1994); W.J.Blyth, S.G.Preston, A.A.Offenberger et al., Phys. Rev. Lett. **74**, 554 (1995).
13. R.K.Janev, L.P.Presnyakov, and V.P.Shevelko, *Physics of Highly Charged Ions*, Ed. by G.Ecker, Springer-Verlag, 1985.
14. A.Fews, P.A.Norreys, F.N.Beg et al., Phys. Rev. Lett. **73**, 1801 (1994).